Quantum Electronics **39** (5) 481 – 486 (2009)

TERAHERTZ RADIATION

PACS numbers: 07.57. – c; 41.60.Cr; 42.30.Ms; 42.30.Va
DOI: 10.1070/QE2009v039n05ABEH013950

Speckle pattern of the images of objects exposed to monochromatic coherent terahertz radiation

N.A. Vinokurov, M.A. Dem'yanenko, D.G. Esaev, B.A. Knyazev, G.N. Kulipanov, O.I. Chashchina, V.S. Cherkassky

***Abstract*. By using a free electron laser and a microbolometer array, real-time images are recorded for the first time in the terahertz range at the rate of up to 90 frames per second. In the case of diffusive illumination of objects by coherent monochromatic radiation, the images consist of speckles. The study of the statistical properties of speckle patterns shows that they are quite accurately described by the theory developed for speckles in the visible range. By averaging a set of images with the help of a rotating scatterer during the exposure time of a frame (20 ms) and by summing statistically independent speckle patterns of many frames, images of the acceptable quality are obtained. The possibilities of terahertz speckle photography and speckle interferometry are discussed.**

Keywords: *terahertz radiation, free electron laser, microbolometer array, images, speckles.*

1. Introduction

Interest in the study of terahertz radiation is caused by several reasons. A low photon energy, not exceeding a few tens of millielectron volts, excludes the ionisation of a medium. Due to a drastic decrease in Rayleigh scattering with increasing wavelength ($\sigma \sim \lambda^{-4}$), terahertz radiation well propagates through turbid media and fine-dispersed materials. The rotational transition frequencies of light molecules, the oscillation frequencies of solid-state plasmas, and the characteristic energies of hydrogen bonds and Van der Walls intermolecular interaction forces lie in the terahertz range. The energy of terahertz photons lies within the energy gap of superconductors. The terahertz range is of great interest for biology and medicine [1] because vibrational frequencies of many biologically important molecules and the activation energy of conformation transitions fall within this range. Because many nonpolar materials are transparent enough for terahertz radiation, the use of this radiation opens up new possibilities for security systems, medical diagnostics, the product quality control, etc. [2 – 4]. One of the most important problems in these and other applications is the imaging of objects in the terahertz range [5, 6].

There is no the general consensus about the boundaries of the terahertz spectral range, and different authors indicate frequency intervals of different widths within 0.1 – 100 THz. If the operation principle of radiation sources is chosen as a criterion, it is reasonable to set the boundaries of the terahertz range equal to 0.5 and 20 THz, which corresponds to wavelengths 600 and 15 μm. Below 0.5 THz, radiation sources are 'electronic' devices such as gyrotrons, orthotrons, and backward-wave oscillators, while radiation sources above 20 THz are thermal sources or lasers. Within the spectral range indicated above, radiation can be generated both by electronic and photonic methods. The breakthrough in the study of terahertz waves was initiated by the invention of broadband femtosecond lasers and the development of time-domain spectroscopy (TDS). Later, monochromatic radiation sources appeared (difference-frequency and parametric oscillators). The review of terahertz radiation sources is presented, for example, in [5].

Until the recent time the power of terahertz radiation sources was in the range from nanowatts to milliwatts [7], and sensitive multichannel detectors were absent. Images were obtained by a prolonged (sometimes, for tens of minutes) scan of an object by a focused terahertz beam [5, 6]. The development of a 50-mW quantum cascade laser [8] and a microbolometer array detector [9] made it possible to record real-time images at the rate of 20 frames per second. The disadvantages of the quantum cascade laser are the necessity of its cooling down to 117 K and the impossibility of frequency tuning. The possibilities of imaging in the terahertz range were considerably expanded after the commission of a repetitively pulsed free electron laser (FEL) in Novosibirsk [10] emitting an average output power of up to 500 W at a pulse repetition rate of 11.2 MHz.

In [11], the highest image recording rate in the terahertz range equal to 90 frames per second was obtained. A radiation source was the FEL, and images were recorded with a microbolometer array detector [12]. Because of a large wavelength, even objects with roughness of 20 – 40 μm are smooth enough, and when they are illuminated by laser radiation with a small divergence, only the elements of the

N.A. Vinokurov, B.A. Knyazev, G.N. Kulipanov G.I. Budker Institute of Nuclear Physics, Siberian Branch, Russian Academy of Sciences, prosp. akad. Lavrent'eva 11, 630090 Novosibirsk, Russia;
e-mail: N.A.Vinokurov@inp.nsk.su;
M.A. Dem'yanenko, D.G. Esaev A.V. Rzhanov Institute of Semiconductor Physics, Siberian Branch, Russian Academy of Sciences, prosp. akad. Lavrent'eva 13, 630090 Novosibirsk, Russia;
e-mail: esaev@thermo.isp.nsc.ru;
O.I. Chashchina, V.S. Cherkassky Novosibirsk State University, ul. Pirogova 2, 63090 Novosibirsk, Russia; e-mail: cherk@phys.nsu.ru

Received 31 July 2008; revision received 14 November 2008
Kvantovaya Elektronika **39** (5) 481 – 486 (2009)
Translated by M.N. Sapozhnikov

object surface whose mirror reflection fell to the solid angle of the optical system appeared in the image. Upon illumination of objects by diffusely scattered radiation, the images of objects consisting of speckles were obtained for the first time in the terahertz range.

The properties of speckles in the visible range have been studied in detail, the methods for improving the image quality have been developed, and measurement methods based on the use of speckles have been elaborated [13–16]. Effects related to the random orientation of coherent radiation were recorded earlier with single-channel detectors as intensity fluctuations in time upon scattering of a terahertz beam in random media [17, 18]. The recording of two-dimensional time-resolved speckle patterns opens up the possibilities for expanding applications of speckle photography, speckle interferometry and other speckle-based methods to the terahertz region. Because the characteristic wavelength in this case is two orders of magnitude higher than that in the visible region, the range of parameters for investigations can be considerably expanded (for example, the value of the object displacement). The transparency of many nonpolar and nonconducting materials for terahertz radiation, which are completely opaque in the visible range, opens up additional possibilities for applications.

2. Experimental

A radiation source was a free electron laser [10] emitting 100-ps pulses with a pulse repetition rate of 5.6 MHz. The laser was continuously tunable from 120 to 240 μm (2.5–1.25 THz) with the relative linewidth of 0.3 %–1 %. All experiments described below were performed at a wavelength of 130 μm. The laser radiation was linearly polarised and spatially coherent. The diameter of the nearly Gaussian laser beam was 50 mm and the beam divergence was 3×10^{-3} rad.

Figure 1a shows the system for imaging in the terahertz range. An object was illuminated either by a narrow laser beam reflected from mirror M1 or radiation scattered by a rough copper foil with inhomogeneities of size exceeding the radiation wavelength. The image of the object was projected with a polyethylene lens on a microbolometer array sensitive in the terahertz range, which contained 160×120 pixels on an area of 8.21×6.1 mm^2. Because of the high sensitivity of the array equal to 1.3×10^{-3} W cm^{-2} [11], the incident radiation was attenuated by rotating a photolithographic polariser mounted at the input [19].

Figure 2a demonstrates an image recorded with the microbolometer array by exposing an object to diffuse terahertz radiation. The object was a 50-Ω BNC T-connector shown in Fig. 2b. One can see that the image of the object consists of rather large speckles. The statistical parameters of speckles were studied by using modified setups shown in Figs 1b, c. In this case, a terahertz radiation beam, whose diameter was controlled with the help of an iris aperture, was incident on a copper scatterer. The scattered radiation was recorded with the array either through a lens (subjective speckles) or directly (objective speckles).

3. Parameters of a speckle pattern

If the roughness of a scatterer is larger than the radiation wavelength, then, according to theory [13], a speckle

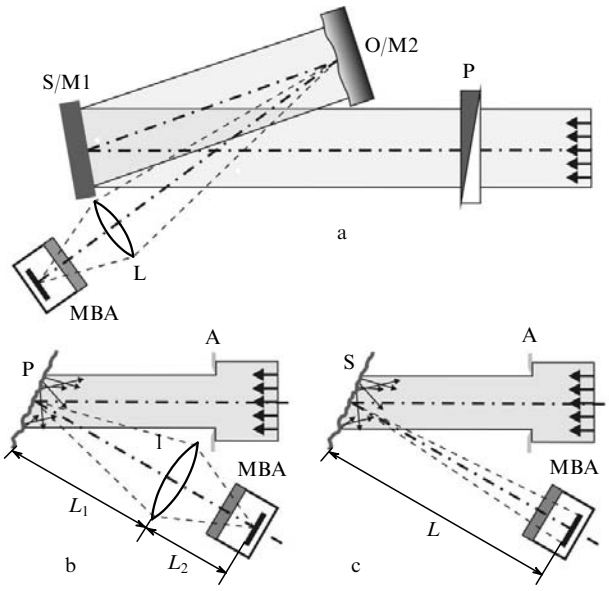

Figure 1. Scheme of the setup for imaging in the terahertz range (a) and its modifications for studying subjective (recording through a lens) (b) and objective (direct recording) (c) speckles: (P) photolithographic polariser; (S) copper foil scatterer; (M1, M2) mirrors; (O) object; (L) polyethylene lens ($f = 54$ mm); (A) iris aperture; (MBA) microbolometer array.

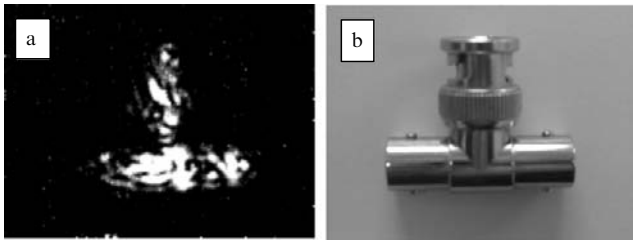

Figure 2. Image of a 50-Ω BNC T-connector obtained with the help of a microbolometer array upon irradiation by a terahertz beam (a) and usual photography (b).

pattern is formed with the intensity probability density described by the Gaussian distribution. It is known that speckles, on the one hand, deteriorate the image quality, and on the other, can be used for metrological purposes, in particular, in speckle photography and speckle interferometry. To use these methods with confidence, it is necessary to make sure experimentally that the statistical properties of speckles observed in our experiments have the same properties as speckles observed in the visible range. For this purpose, we performed three series of measurements. First we 'photographed objective and subjective speckles with the microbolometer array by varying the diameter D of an incident terahertz beam from 5 to 30 mm for constant L, L_1, and L_2 (Fig. 1), and then – objective speckle patterns, by varying the distance L from a scatterer to the array within 103–110 mm for a constant diameter D of the terahertz illuminating a scatterer. In this section, we present the results of analysis of twenty-three images containing 0.44 millions of pixels. Three speckle patterns are shown in Fig. 3.

As expected, the characteristic size b_s of objective speckles (Figs 3a, b) changed inversely proportional to the terahertz beam diameter [20, p. 35]:

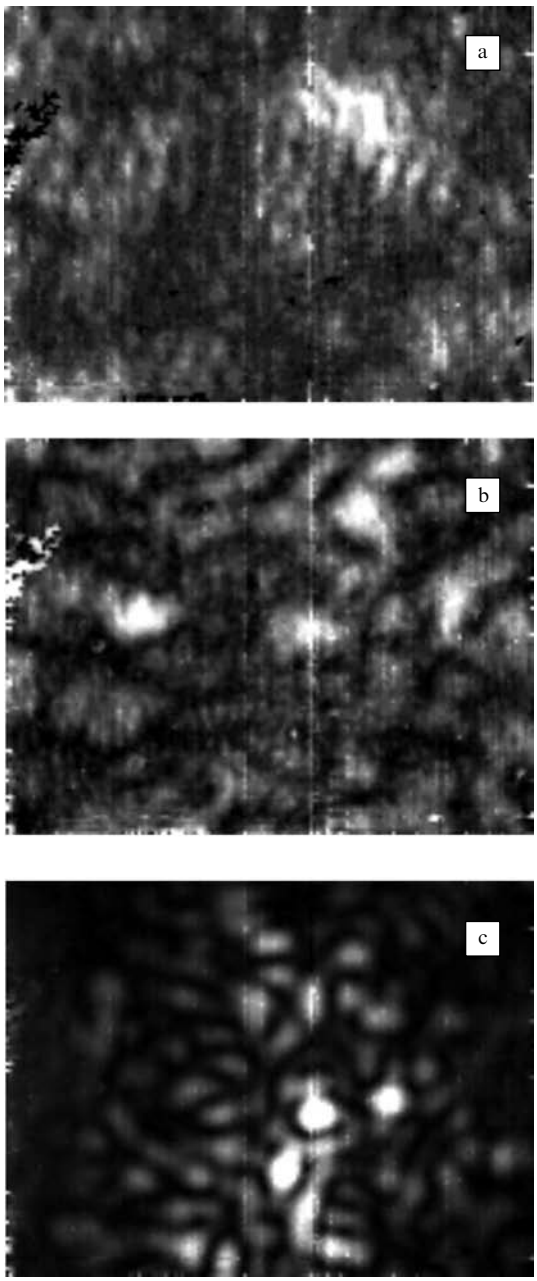

Figure 3. Spectra recorded with a microbolometer array for 20 ms by irradiating a scatterer by terahertz beams of different diameters D: objective speckles for $D = 13$ (a) and 30 mm (b), and subjective speckles for $D = 10$ mm (c).

$$b_s \approx 1.5(\lambda L/D), \tag{1}$$

where λ is the radiation wavelength and L is the distance from the scatterer to the recording plane. According to the theory, the characteristic theoretical size of subjective speckles

$$b_s \approx 1.22(\lambda L_1/d), \tag{2}$$

(where L_1 is the distance from the scatterer to the lens and d is the lens diameter) was independent of the incident beam diameter, and the speckle pattern remained almost invariable with changing the beam diameter (Fig. 3c).

The intensity distribution in small speckles well corresponded to the theoretical distribution

$$I(y) = 1 + \cos\left[2\pi\left(\frac{\Delta y}{3\lambda z}\right)\right]. \tag{3}$$

Here, y is the coordinate measured from a speckle centre, and Δ and z correspond to D and L (for objective speckles) and d and L_1 (for subjective speckles). The experimental intensity distribution measured for one of the speckles is shown by dots in Fig. 4a (the solid curve is the fit of the experimental data by a function of the type 'unity + cosine'). The image of large speckles was distorted by a rather regular small-scale interference, but the total size of spots also well corresponded to the theoretical size. The origin of the small-scale interference is not clear so far. The analysis of all images showed (Fig. 4b) that the dependence of the size of spots (full width at half-maximum) on the aperture Δ is close to theoretical values (1) and (2).

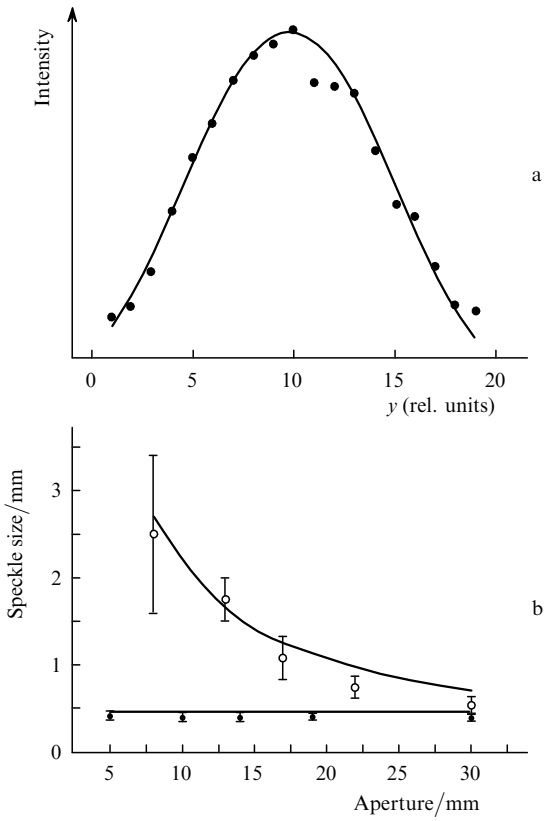

Figure 4. Intensity distribution over an objective speckle section for $D =$ 22 mm (a) and characteristic sizes of subjective (●) and objective (b) speckles as functions of the diameter of a terahertz beam on a scatterer (○).

Because the characteristic size of inhomogeneities of the scatterer greatly exceeded the radiation wavelength, we could expect that a developed speckle pattern will be observed under our conditions. A specific feature of such a speckle pattern is the Gaussian intensity distribution in it. The intensity distribution histograms for all 23 frames constructed after the displacement of zero by the value of the background illumination and noise were close to the typical histogram shown in Fig. 5 (subjective speckle pattern for $L_1 = 106$ mm and $d = 40$ mm). Indeed, the main part of experimental data corresponds to the Gaussian distribution

(the solid line in Fig. 5). According to theory [13, p. 18], in the case of the developed speckle pattern, the exponentially decaying dependence should start at the zero intensity. In our case, however, the instant intensity distribution density decreases at low intensities. This can be explained by several reasons. First, the microbolometer array, having the maximum sensitivity in the region 10–14 μm, recorded extraneous background emission, which was inhomogeneous over the field. The plot was constructed by subtracting first from the radiation intensity the value providing the beginning of the probability density histogram at the zero intensity. Obviously, this produces distortions in the intensity distribution in the region of low intensities. Second, the detector noise can lead to the same effect (see Fig. 2 in [21]). Third, due to internal reflection from the input window of the array, the array recorded in each frame the superposition of at least two beams. Because the delay of one beam with respect to another $\tau_{12} = nl/c \approx 55$ ps (nl is the optical thickness of the germanium window of the array) is close to the laser pulse duration, we can assume that the superposition of two speckle patterns occurs (the summation of their intensities). The superposition of two speckle patterns, if the linear correlation coefficient between them is not unity, also reduces the intensity distribution density to zero at the coordinate origin [13, p. 24]. Note, however, that the deviation from a Gaussian in our case can be considered small because the criterion characterising the closeness of a function to a Gaussian, namely, the contrast of the speckle pattern

$$C = \frac{\sigma_I}{\langle I \rangle} = \frac{\left(\langle I^2 \rangle - \langle I \rangle^2\right)^{1/2}}{\langle I \rangle} \tag{4}$$

proved to be 1.04 ± 0.03 for all frames (the theoretical value is $C = 1$). Thus, first-order statistical characteristics demonstrate that speckles in the terahertz range have usual properties, and the speckle pattern in our case can be considered well developed.

Consider now second-order statistical characteristics. We can calculate the cross-correlation Pearson coefficient

$$c_{kl} = \frac{\langle I_k I_l \rangle - \langle I_k \rangle \langle I_l \rangle}{\left[\left\langle \left(I_k - \langle I_k \rangle\right)^2 \right\rangle \left\langle \left(I_l - \langle I_l \rangle\right)^2 \right\rangle\right]^{1/2}} \tag{5}$$

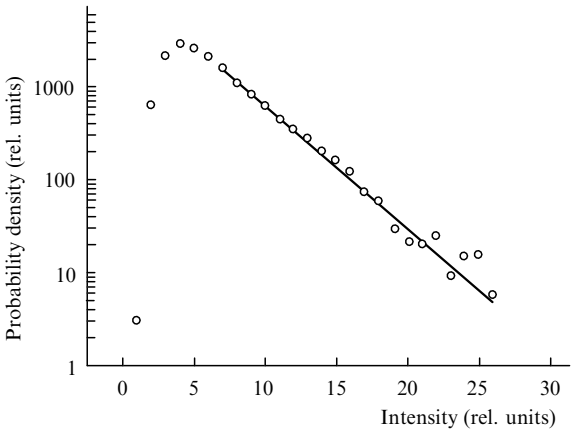

Figure 5. Distribution of the instant intensity density over the array pixels in a speckle pattern recorded upon successive reflections of a terahertz beam from a scatterer S and mirror M2 in the setup shown in Fig. 1a.

from our experiments for any pair of frames k and l chosen from the two sets of speckles patterns. As the recording plane is moved away from a scatterer, the correlation between objective speckles is preserved, according to theory [14, p. 30], as long as the displacement δz of the recording plane satisfies the condition $\delta z < 8\lambda L^2/D^2$. Cross-correlation coefficients for eight pairs of frames recorded with the microbolometer array for the diameter of the illuminated region of the scatterer $D = 30$ mm are presented in Fig. 6a. Each point corresponds to the cross-correlation coefficient for a frame recorded at a distance indicated on the ordinate and a frame recorded at a distance of 103 mm. One can see that the cross-correlation coefficient becomes equal to 0.5 when the recording plane is displaced by 5 mm, whereas $8\lambda L^2/D^2 = 13$ mm, which satisfies the condition presented above.

The subjective speckle pattern at the invariable diameter of a lens should not depend on the diameter of the illuminated region of a scatterer [13, 14]. To verify the correctness of this statement, we calculated the cross-correlation coefficient (Fig. 6b) for a sequence of frames recorded at the fixed positions of the lens and microbolometer array, but different diameters of a terahertz radiation spot on a scatterer. One can see that, as the spot diameter is increased by six times, the correlation coefficient remains close to unity with good accuracy. A systematic decrease in c_{kl} by 20 % with increasing diameter is most likely explained by the decrease in the terahertz beam intensity at the periphery (the beam half-width is ~ 40 mm) and a weak inhomogeneity of the beam. Thus, both the first- and second-order statistical characteristics in the terahertz frequency range correspond to theoretical expectations.

4. Image quality improvement

As follows from expressions (1) and (2), images obtained upon diffusion illumination of objects by coherent terahertz radiation consist of large speckles, which are two hundreds

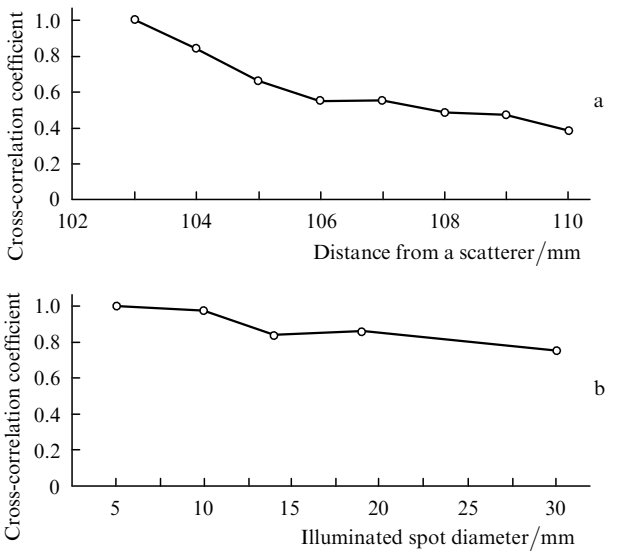

Figure 6. Cross-correlation Pearson coefficients calculated for a set of frame pairs corresponding to the displacement of the speckle recording plane along the optical axis in the setup in Fig. 1c (a) and the change in the diameter of the illuminated region of the scatterer (Fig. 1b) (b).

times larger than usual speckles observed in the visible range. For this reason, the images of objects are formed by a small number of speckles, and the image quality is very poor. This is demonstrated, for example, by the image of a metal key recorded with a microbolometer array (Fig. 7, frame 73). It is very difficult to identify an object in this frame. Obviously, to obtain a better image, it is necessary to use special methods, which are well known for the visible range. They are described in detail in [22] and many other papers.

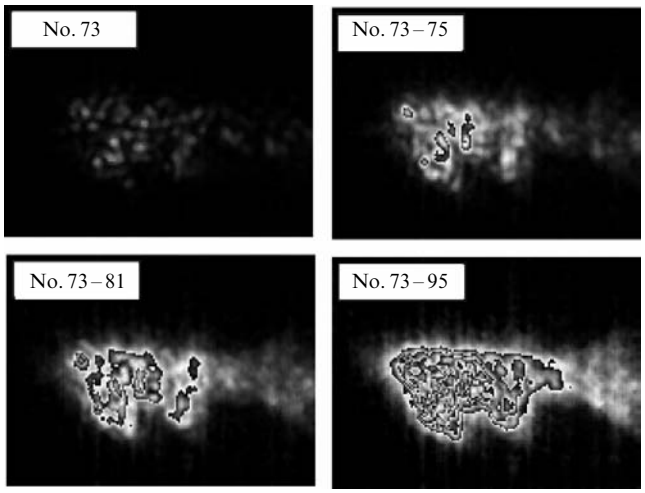

Figure 7. Images of a metal key barb illuminated by a diffuse terahertz beam obtained for the exposure time of 1/90 s in one frame (frame No. 73) and upon the superposition of three, nine, and twenty-three frames with uncorrelated speckle patterns.

One of the methods of speckle metrology is the superposition of speckle patterns obtained by displacing mutually the illuminating beam and object. Figure 7 presents images obtained by the superpositions of three, nine, and twenty-three frames taken by rotating the scatterer successively by an angle providing the loss of correlation between the patterns. One can see that the last image is already distinct enough. The disadvantages of this method are a considerable decrease in the image recording rate and the deterioration of spatial resolution when the number of frames is not large enough. A considerably more efficient is the method based on a very rapid rotation of a scatterer, which provides the averaging of speckle patterns during the exposure of one frame. This method gives real-time images with the rate of up to 90 frames per second (see Fig. 4 in [11]) with the spatial resolution close to the wave limit.

5. Conclusions

Speckle patterns of images obtained by exposing objects to monochromatic coherent terahertz radiation are well described by the classical theory developed by Goodman. By using high-power radiation sources and highly sensitive multichannel image detectors with a high recording rate, it is possible to obtain high-quality real-time images by superimposing a great number of speckle patterns in one way or another, which considerably expands the possibilities of application of terahertz imaging devices in security systems and biomedical, industrial and other fields.

Being, on the one hand, the reason for the deterioration of the image quality, speckles, on the other hand, can be used for speckle metrology [23, p. 103], often simplifying considerably the measurement technique. Our paper opens up the possibility of expanding speckle photography and speckle interferometry to the terahertz frequency range. A greater wavelength of terahertz radiation allows the measurement of displacements and deformations that are two orders of magnitudes larger than those measured in the visible range. Because terahertz radiation is transmitted by many materials, which are opaque for visible radiation (paper, cardboard, some plastics and tissues, and many other nonpolar materials), it is possible to develop new methods for recording hidden objects. The results of experiments demonstrating the possibilities of terahertz speckle photography and speckle interferometry will be published elsewhere.

Acknowledgements. This work was partially supported by the Program P-05 of Fundamental Studies of the Presidium of the Russian Academy of Sciences, the Integration Grants of the Siberian Branch, RAS (Grant Nos 174/6 and 22/6), the Russian Foundation for Basic Research (Grant No. 07-02-13547), and the Ministry of Education and Science of the Russian Federation (Grant RNP.2.1.1.3846). The authors thank V.V. Kotenkov, V.V. Kubarev, A.N. Matveenko, T.V. Salikova, S.S. Serednyakov, O.A. Shevchenko, and M.A. Shcheglov for their assistance with the experiments and fruitful discussions.

References

1. Pickwell E., Wallace V.P. *J. Phys. D: Appl. Phys.*, **39**, R301 (2006).
2. Fischer B., Hoffmann N., Helm H., et al. *Semicond. Sci. Technol*, **20**, S246 (2005).
3. Leahy-Hoppa M.R., Fitch M.J., Zheng X., et al. *Chem. Phys. Lett.*, **434**, 227 (2007).
4. Nischizawa J., Sasaki T., Suto K., et al. *Opt. Commun.*, **244**, 469 (2005).
5. Mickan S.P., Zhang X.-C. *Intern. J. High Speed Electron. Syst.*, **13**, 601 (2003).
6. Chan W.L., Daibel J., Mittelman D.M. *Rep. Prog. Phys.*, **70**, 1325 (2007).
7. Cooke M. *Semiconductor Today: Compounds and Advances Silicon*, **2**, 39 (2007).
8. Hu Q., Williams B.S., Kumar S., et al. *Semicond. Sci. Technol.*, **20**, S228 (2005).
9. Lee A., Williams B.S., Kumar S., et al. *IEEE Photon. Technol. Lett.*, **18**, 1415 (2006).
10. Gavrilov N.G., Knyazev B.A., Kolobanov E.I., et al. *Nucl. Instrum. Methods in Phys. Research A*, **575**, 54 (2007).
11. Dem'yanenko M.A., Esaev D.G., Knyazev B.A., et al. *Appl. Phys. Lett.*, **92**, 131116 (2008).
12. Dem'yanenko M.A., Ovsyuk V.N., Shashkin V.V., et al. *Proc. SPIE Int. Soc. Opt. Eng.*, **5957**, 340 (2005).
13. Goodman J.W., in *Laser Speckle and Related Phenomena.* Ed. by J.C. Dainty (New York: Springer-Verlag, 1975) p. 9.
14. Francon M. *Laser Speckle and Applications in Optics* (New York: Academic Press, 1979; Moscow: Mir, 1980).
15. Klimenko I.S. *Golografiya strukturnykh izobrazhenii i spekl-interferometriya* (Holography of Structural Images and Speckle Interferometry) (Moscow: Nauka, 1985).
16. Zel'dovich B.Ya., Shkunov V.V., Yakovleva T.V. *Usp. Fiz. Nauk*, **149**, 511 (1986).
17. Jian Z., Pearce J., Mittelman D.M. *Phys. Rev. Lett.*, **91**, 033903 (2003).
18. Pearce J., Doyle K., Jian Z., Deibel J., Mittelman D.M. *J. Opt. Soc. Am. B*, **23**, 1506 (2006).

19. Cherkassky V.S., Knyazev B.A., Kulipanov G.N., et al. *Intern. J. Infrared and Millimeter Waves*, **28**, 219 (2007).
20. Vest C.M. *Holographic Interferometry* (New York: John Wiley, 1979).
21. Apostol A., Dogariu A. *Opt. Lett.*, **29**, 235 (2004).
22. McKechnie T., in *Laser Speckle and Related Phenomena.* Ed. by J.C. Dainty (New York: Springer-Verlag, 1975) p. 123.
23. Rastogi P.K. *Photomechanics. Topics Appl. Phys.*, **77**, 103 (2000).